Katunuma, N., Mikumo, K., Matsuda, M., & Okada, M. (1962) *J. Vitaminol. 8*, 68–73.
Klarskov, K., Breddam, K., & Roepstorff, P. (1989) *Anal. Biochem. 180*, 28–37.
Klotz, I. M. (1967) *Methods Enzymol. 11*, 576–580.
Landon, M. (1977) *Methods Enzymol. 47*, 145–149.
Mahoney, W. C., & Hermodson, M. A. (1980) *J. Biol. Chem. 255*, 11199–11203.
Martini, F., Angelaccio, S., Barra, D., Pascarella, S., Maras, B., Doonan, S., & Bossa, F. (1985) *Biochim. Biophys. Acta 832*, 46–51.
Masaki, T., Tanabe, M., Nakamura, K., & Soejima, M. (1981) *Biochim. Biophys. Acta 660*, 44–50.
Matsuzawa, T., & Segal, H. L. (1968) *J. Biol. Chem. 243*, 5929–5934.
Noguchi, T., Takada, Y. & Kido, R. (1977) *Hoppe-Seyler's Z. Physiol. Chem. 358*, 1533–1542.
Omenn, G. S., Fontana, A., & Anfinsen, C. B. (1970) *J. Biol. Chem. 245*, 1895–1902.
Roepstorff, P., Nielsen, P. F., Klarskov, K., & Hejrup, P. (1988) *Biomed. Environ. Mass Spectrom. 16*, 9–18.
Ruegg, U., & Rudinger, J. (1977) *Methods Enzymol. 47*, 111–116.
Saha, N., & Bhattacharyya, S. P. (1989) *Hum. Hered. 39*, 110–112.
Skoog, B., & Wichman, A. (1986) *Trends Anal. Chem. 5*, 82–83.
Titani, K., & Narita, K. (1964) *J. Biochem. (Tokyo) 56*, 241–265.
Tsunasawa, S., & Narita, K. (1976) *Methods Enzymol. 45*, 552–561.
Ueda, S., Omoto, K., Park, K. S., & Kudo, T. (1979) *Hum. Hered. 29*, 208–212.

Assignment of the Natural Abundance ^{13}C Spectrum of Proteins Using ^{13}C ^{1}H-Detected Heteronuclear Multiple-Bond Correlation NMR Spectroscopy: Structural Information and Stereospecific Assignments from Two- and Three-Bond Carbon–Hydrogen Coupling Constants†

Poul Erik Hansen
Institute for Life Sciences and Chemistry, Roskilde University, P. O. Box 260, DK-4000 Roskilde, Denmark
Received May 23, 1991; Revised Manuscript Received August 7, 1991

ABSTRACT: Proton-detected heteronuclear multiple-bond ^{1}H–^{13}C correlations (HMBC) previously have been used for assignment purposes in a variety of isotopically enriched proteins. In the present study it is demonstrated that the technique yields an almost complete assignment of the natural abundance ^{13}C spectrum of the protein basic pancreatic trypsin inhibitor (BPTI). In addition, the technique permits additional ^{1}H assignments to be made for this well-studied protein. The intensities of observed correlations permit rough estimates to be made of $^{2}J(C,H)$ and $^{3}J(C,H)$ coupling constants. These couplings can be used for conformational studies of both the side chains and the backbone. Intra- and interresidue coupling between CαH and the carbonyl carbon provides information about the backbone angles ψ and ϕ. Side-chain conformations can be determined from both two- and three-bond carbon–hydrogen coupling constants. The present study of BPTI together with its known high-precision solution structure yields an experimental correlation between resonance intensities and secondary structure. The spectra show the potential of the method in analyzing ^{13}C NMR spectra of nonenriched proteins. The method yields ^{13}C NMR chemical shifts, which are versatile parameters to be used to monitor structural changes, titrations, etc.

Determination of solution structures of proteins by ^{1}H NMR[1] has reached a high degree of refinement (Wüthrich, 1986, 1989; Clore & Gronenborn, 1987, 1989; Bax, 1989). At present, interproton distance constraints derived from NOE spectra and dihedral angles derived from ^{1}H–^{1}H couplings are the only observables used in the structure determination process. In the present paper we explore the use of ^{1}H-detected heteronuclear multiple-bond connectivity (HMBC) to obtain qualitative estimates for a third type of parameter, ^{1}H–^{13}C long-range coupling $^{n}J(C,H)$. These couplings provide a rich source of additional conformational information, not yet thoroughly explored for protein structure determination.

For obtaining the highest quality structure, it is important to obtain stereospecific assignments (Guntert et al., 1989; Driscoll et al., 1989). Stereospecific assignments of a significant fraction of the Cβ methylene protons can often be obtained by using a combination of NOE and $J(H,H)$ coupling information, possibly combined with the search of a data bank. As is well known from model peptide studies, $J(C,H)$ couplings combined with $J(H,H)$ information often also provide sufficient unambiguous information to make such stereospecific assignments. In particular, three-bond $^{3}J(C',H\beta)$ couplings in conjunction with $^{3}J(H\alpha,H\beta)$ couplings can be used to make stereospecific assignments of Cβ methylene protons (Hansen et al., 1975; Cowburn et al., 1983). In addition, the interre-

†Support from the Danish Natural Science Research Council is greatly appreciated.

[1] Abbreviations: BPTI, basic pancreatic trypsin inhibitor; γ, gyromagnetic ratio; HOHAHA, Homonuclear Hartmann–Hahn; NOE, nuclear Overhauser enhancement; NMR, nuclear magnetic resonance; T_1, spin–lattice relaxation time; T_2, spin–spin relation time; HMBC, ^{1}H-detected heteronuclear multiple-bond correlation.

0006-2960/91/0430-10457$02.50/0 © 1991 American Chemical Society

sidue $^3J(C',N,H\alpha)$ coupling provides information about the ϕ angle (Bystrov, 1975; Hansen et al., 1975). J(C,H) couplings can also provide information about amino acid side-chain information that sometimes may be difficult to obtain with the standard NMR approaches, particularly for side chains that exhibit internal rotations.

^1H–^{13}C multiple-bond connectivity can also be very helpful for assignment purposes, as demonstrated for a number of peptides (Kessler et al., 1988a,b; Bermel et al., 1989), proteins (Kessler et al., 1990), and isotopically labeled proteins (Markley et al., 1988; Bax et al., 1988). For example, since a backbone carbonyl may show HMBC correlation with the two adjacent CαH protons, these correlations provide an unambiguous method for sequential assignment of the ^1H spectrum. The strength of the HMBC technique lies in the multitude of long-range correlations that can be observed for each carbon. For most carbons at least two and often three of four long-range correlations can be observed. The ^{13}C assignment is therefore easily done by correlation with assigned ^1H resonances, even in the case of severe ^1H resonance overlap.

The ^1H-detected HMBC technique (Bax & Summers, 1986) is the most sensitive general NMR method for observing such long-range correlations, and the experiment is preferably conducted in a mixed mode, with absorption in the ^{13}C dimension and absolute value in the ^1H dimension (Bax & Marion, 1988). However, as recently demonstrated (Davis, 1989), recording a fully phase-sensitive version of the spectrum may have advantages in some cases. In principle, it is possible to extract quantitative J coupling information from the HMBC spectrum (Bermel et al., 1989). Unfortunately, in practice we find in our protein studies that the signal-to-noise ratio is far too low to permit such a quantitative measurement.

Our present investigation of the use of heteronuclear multiple-bond ^1H–^{13}C correlations focuses on the basic pancreatic trypsin inhibitor (BPTI). This choice is made because of its high solubility and stability and because of the extensive number of both structural (Deisenhofer & Steigeman, 1975; Wlodawer et al., 1984, 1987) and ^1H NMR studies (Wüthrich, 1989; Wagner et al., 1987; Wagner & Wüthrich, 1982) of this protein. Partial assignments of the ^{13}C spectrum of BPTI have been published. The Cα carbons have been assigned almost completely (Wagner & Brühweiler, 1987), and the carbonyl region has been assigned to a large extent (Tüchsen & Hansen, 1988). As will be shown in our present study, the HMBC experiment not only provides nearly complete assignments of the ^{13}C NMR spectrum, it also yields several new ^1H assignments of this previously well-studied protein.

Materials and Methods

HMBC spectra were recorded at 500 MHz ^1H frequency on a Bruker AM-500 spectrometer, using a 11 mM solution of BPTI in 99.96% D_2O, p^{2}H 5.3, and 100 mM NaCl. HMBC spectra were recorded at 47 and 61 °C, using a 9.5-μs ^1H 90° pulse width and a 10.5-μs ^{13}C 90° pulse width. HMBC spectra result from 1024 × 1024 data matrices, corresponding to data acquisition times of 22.5 ms (t_1) and 102 ms (t_2). The delay time between scans was 1.3 s, and 128 scans were acquired per t_1 duration, yielding total measuring times of 48 h per 2D spectrum. Data were processed following the mixed-mode recipe (Bax & Marion, 1988), with absorption in the ^{13}C dimension and absolute value in the ^1H dimension. Filtering with an unshifted sine bell was used in the F_2 dimension; Lorentzian line narrowing (−15 Hz) combined with Gaussian broadening (+25 Hz) were used in the F_1 dimension. Zero filling was used to yield a final digital resolution of 22 Hz (F_1) and 5 Hz (F_2). For quantification purposes, data were also processed as described above, but utilizing only the first 700 t_2 data points, limiting the effective t_2 acquisition time to 70 ms, and using an unshifted sine bell filtering function for this portion of the signal.

The fixed delay time, Δ_2, in the 90(^1H)–Δ_2–90(^{13}C)–$t_1/2$–180(^1H)–$t_1/2$–90(^{13}C)–acquire pulse scheme was set to 35 and 38 ms in the experiments recorded at 61 and 47 °C, respectively. The Δ_2 delays were chosen slightly different in the two experiments to maximize the number of one-bond couplings that could be observed. Note that no one-bond connectivity is observed if Δ_2 accidentally equals $[Nx^1J(C,H)]^{-1}$.

Results

The intensity of a particular correlation in a HMBC spectrum depends on the magnitude of the long range J(C,H) coupling constant, on the homonuclear proton couplings J(H,H), and on the ^1H transverse relaxation time, T_2, and can be described by the equation (Clore et al., 1988)

$$s(t_1,t_2) = \exp[-(\Delta_2 + t_1 + t_2)/T_2] \sin(\pi J_{CH}\Delta_2) \sin(J_{CH}t_2)\Pi[\cos[\pi J_{Hk}(\Delta_2 + t_1 + t_2)]] \quad (1)$$

where J_{Hk} is the homonuclear coupling between proton k and the proton observed in the long range correlation.

As can be seen in the HMBC spectrum shown in Figure 1, correlations normally appear as singlets. This results from the fact that usually neither the heteronuclear coupling J(C,H) nor the passive homonuclear couplings J_{Hk} can be fully resolved in the ^1H dimension which shows absolute value mode line shapes. Correlations via one-bond J_{CH} couplings are an exception to this rule, and they appear as doublets with a separation equal to ^1J(C,H). Poorly resolved homonuclear couplings can be seen for a large number of HMBC correlations to protons that have a single dominating J_{HH} coupling. For example, all correlations to glycines show this pattern (with the exception of Gly-56, for which the two α-protons are degenerate). For Asx residues, correlations from Cγ to the Cβ proton that is gauche with respect to CαH show a similar partially resolved splitting, thus making the Hβ_2–Hβ_3 coupling the dominant one. In addition, some of the CαH resonances show signs of broadening or partially resolved splittings in the F_2 dimension of the HMBC spectrum. The variation in the proton multiplet patterns plus the differences in proton T_2 values make it difficult to quantify the intensities in a rigorous manner. However, in our experiments we have kept the delay Δ_2 and the durations of the acquisition times t_1 and t_2 all relatively short, in order to minimize these effects, albeit at some cost in sensitivity. For quatification purposes, the t_2 acquisition time was made short in an artificial manner by only processing the first 70 ms of the acquired data, allowing more reliable intensity measurements. Since under these conditions resonance intensities show a nearly quadratic dependence on the size of the long-range J_{CH} coupling (eq 1), classification of the correlation intensities in a qualitative fashion is still useful. We distinguish four different intensities: strong, medium, weak, and absent. A more quantitative analysis is possible when all homonuclear proton couplings and the proton T_2 are known (by using eq 1) or when long-range couplings to a single proton are compared relative to one another. For example, when a particular CαH proton shows correlations to two carbonyl carbons and to its own Cβ and Cγ carbons, all correlation intensities are influenced in the same manner by the unknown parameters.

Assignment of the HMBC spectra is made on the basis of the known ^1H chemical shifts (Wagner & Wüthrich, 1982; Wagner et al., 1987). Even though there is substantial overlap in the ^1H spectrum, unambiguous assignment of the ^{13}C

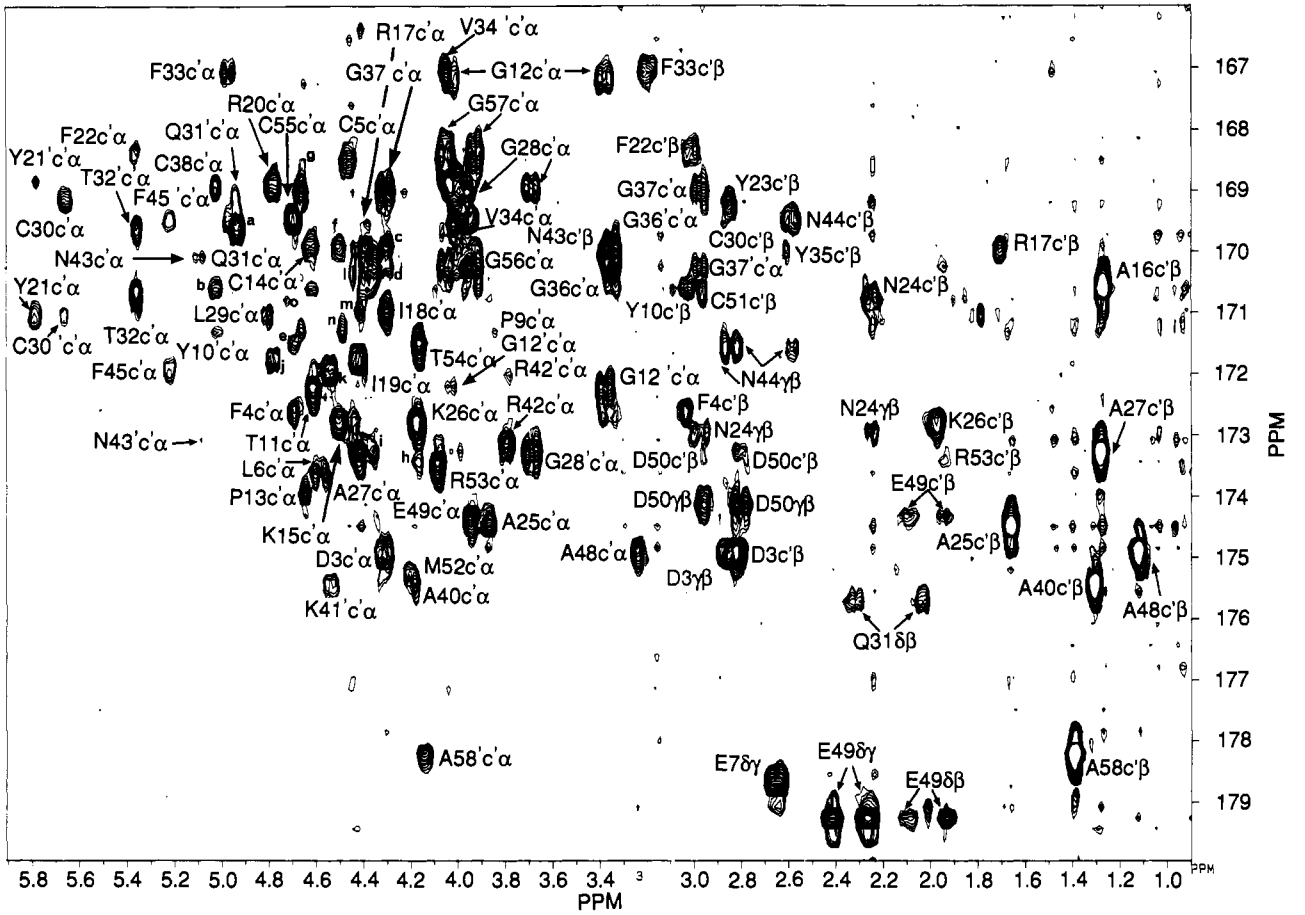

FIGURE 1: HMBC NMR natural abundance spectrum of the carbonyl region of BPTI recorded at 61 °C. TSP served as internal reference. Residues are marked according to type, residue number, and type of hydrogen used for detection. A prime indicates a resonance of R′(C′,Hα) type. Letters: a, N44C′α; b, Y10C′α; c, I18′C′α; d, G36C′α; e, C55C′α; f, K15′C′α; g, S47C′α; h, T54C′α; i, D50C′α; j, R20C′α; k, K41C′α; l, A16C′α; m, I19C′α; n, K46C′α; o, N24C′α.

correlations is often possible because multiple correlations usually are observed for a particular carbon.

The pattern due to poorly resolved homonuclear couplings may also be of use in the assignment, as this pattern will occur at several resonances detected via the same proton, e.g., Phe-33 shows this effect at R(C′,Hα) and R′(C′,Hα).

In these discussions, R(C*x*,H*y*) refers to a resonance due to a correlation between carbon C*x* and proton H*y*. Interresidue correlations between CαH of one residue and the carbonyl of the proceding one are denoted by R′(C′,Hα); intraresidue C=O Hα connectivity is denoted by R(C′,Hα). Through out the paper the rotamer notation of Wagner et al. (1987) is used (see also Figure 6A).

Carbonyl Assignments. Two-bond R(C′,Hα) connectivities are observed for all residues except Pro-2, Pro-8, Tyr-23, and Tyr-35 (Figure 1). However, the carbonyl shifts for Tyr-23 and Tyr-35 can be determined from R(C′,Hβ) connectivities, present in Figure 1. Correlations for Glu-7, Val-34, and Arg-39 could not be determined with certainty because of overlap. The carbonyl assignments obtained from the spectrum of Figure 1 are given in Table S1 in the Supplementary Material. When accounting for differences in temperature, pH, and ionic strength, these values agree largely with values reported by Tüchsen and Hansen (1988) (Table S1, Supplementary Material).

The variation in intensities of the R(C′,Hα) correlations is one of the most conspicuous features of the HMBC spectrum shown in Figure 1. This variation spans from some resonances not detected at all and others barely visible (e.g., Pro-9 and Asn-24) to resonances of glycines that generally are strong. The same is true for Ile, Thr, and Val residues. Since for these residues the CαH proton has only one scalar coupling partner, intensities are expected to be, on average, higher than for residues with two Hβ methylene protons (eq 1).

A comparison of dihedral O–C–C–Hα angle ($\psi + 60°$) as taken from the neutron diffraction structure (Wlodawer, 1987) and the intensities of R(C′,Hα) of residues with two Cβ methylene protons appears to show that the intensities on average correlate with the dihedral angle; the ^2J(C′,Hα) appear to be weakest when the dihedral angle is near 180°, i.e., $\psi = 120°$.

Intraresidue three-bond correlations, R(C′,Hβ), show a large variation in intensity. They are strong for alanines, as expected because three protons observe a single carbon resonance (Bax & Lerner, 1986) and also because the multiplet width of the Ala methyl groups is narrow, J(Hα,Hβ) ~ 7 Hz. R(C′,Hβ) resonances are too weak to be observed for type 3 residues, and for type 1 and type 2 residues only one resonance is observed in accord with the expected values of couplings close to 1 and 11.6 Hz for gauche and trans geometries (Hansen et al., 1975; Espersen & Martin, 1976; Cowburn et al., 1983).

Three-bond coupling via the peptide bond are usually smaller than ^3J(C′,Hβ) couplings (Bystrov, 1976), and correspondingly most of the R′(C′,Hα) connectivities are relatively weak. As found previously for the protein staphylococcal nuclease (Bax et al., 1988) the most intense correlations are observed when $\phi = 180°$, resulting in a cis arrangement of Hα and C′.

Figure 1 also shows connectivities to Cγ and Cδ side-chain carbonyl resonances of Asx and Glu residues, yielding as-

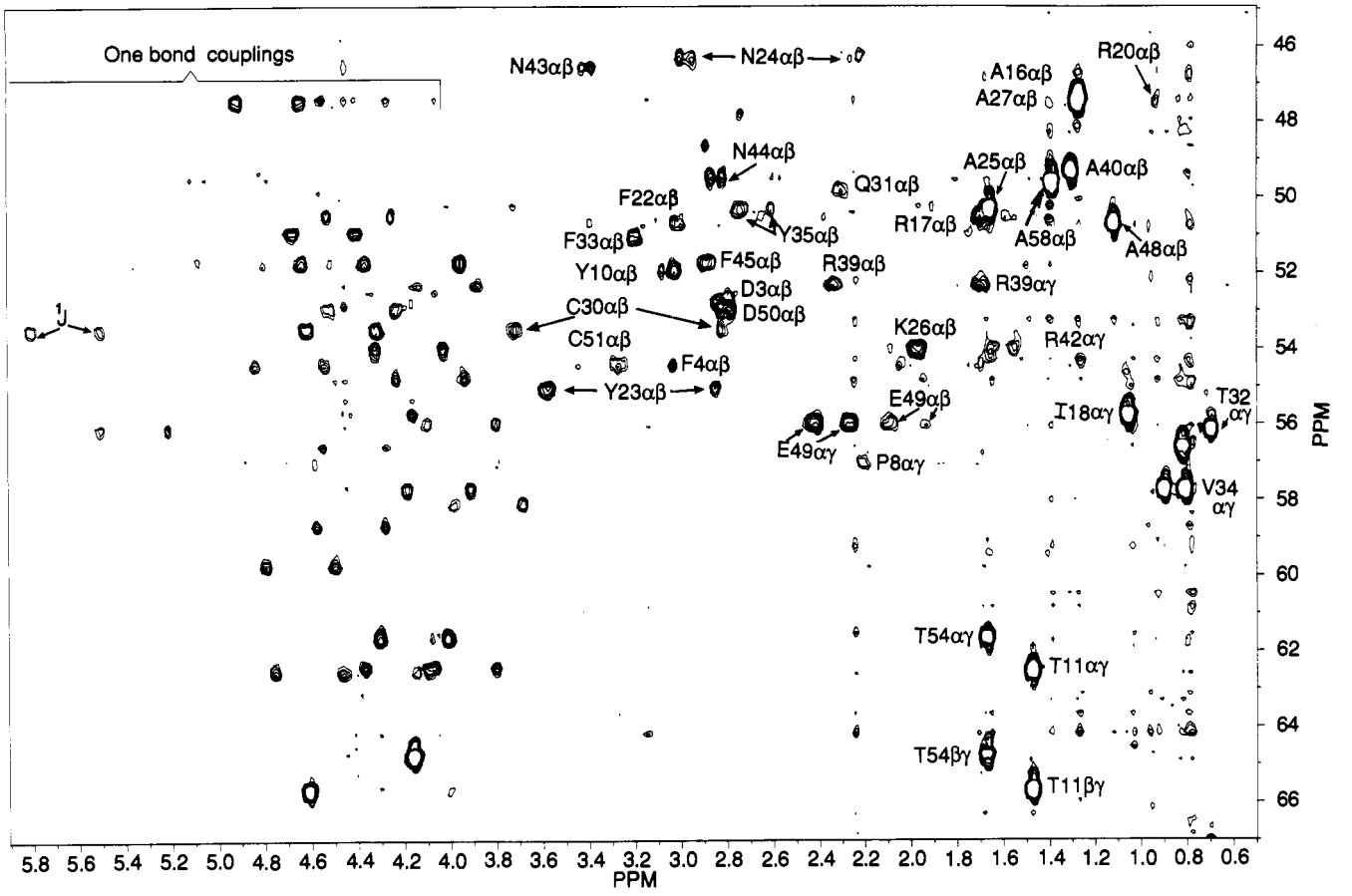

FIGURE 2: HMBC NMR natural abundance spectrum of BPTI. Aliphatic part of the spectrum showing Cα carbons. Δ_2 = 35 ms.

signment information for these important side-chain reporter groups.

Cα Assignments. Nearly complete assignments of the Cα carbons have previously been reported by Wagner and Brühweiler (1986). On the basis of their one-bond J correlation, the Cα resonances of Phe-4 and Gln-7 and those of Phe-33 and Tyr-35 could not be distinguished. These ambiguities are resolved by inspection of region of the HMBC spectrum which shows correlation to these Cα carbons (Figure 2). When considering both correlation spectra, recorded with Δ_2 values of 35 and 38 ms, all correlations due to $^1J(C\alpha,H\alpha)$ are also observed in this spectral region except for Tyr-21. A total of 23 of the assignments based on $^1J(C\alpha,H\alpha)$, including that of Tyr-21, are supported by the observation of R(Cα,Hβ) and R(Cα,Hγ) connectivities.

The $^1J(C\alpha,H\alpha)$ coupling constants measured from the observed splittings in Figure 2 fall in the range from 130 to 154 (±5) Hz. Arg-39 has the smallest one-bond coupling, and Pro-13 and Cys-14 have the largest coupling.

Cβ Assignments. On the basis of the HMBC spectra, it was possible to make complete assignment of the Cβ carbons except those of Cys-38 and Arg-1. Our assignment of Cys-51 Cβ is tentative. Our assignments confirm the partial assignment reported by Brühweihler and Wagner (1986). Results are summarized in Table S2 (Supplementary Material) and Figure 3. As was the case for the Cα resonances, for many Cβ carbons the one-bond correlations are confirmed by long-range correlations due to CαH, CγH, or CδH resonances.

Assignment of Other Side-Chain Carbons. Assignment of the side-chain carbons beyond Cβ can be divided into two parts, depending on the type of side chain (aromatic or aliphatic). Completely analogous to the assignment of the Cα and Cβ resonances, the remaining aliphatic side-chain carbon

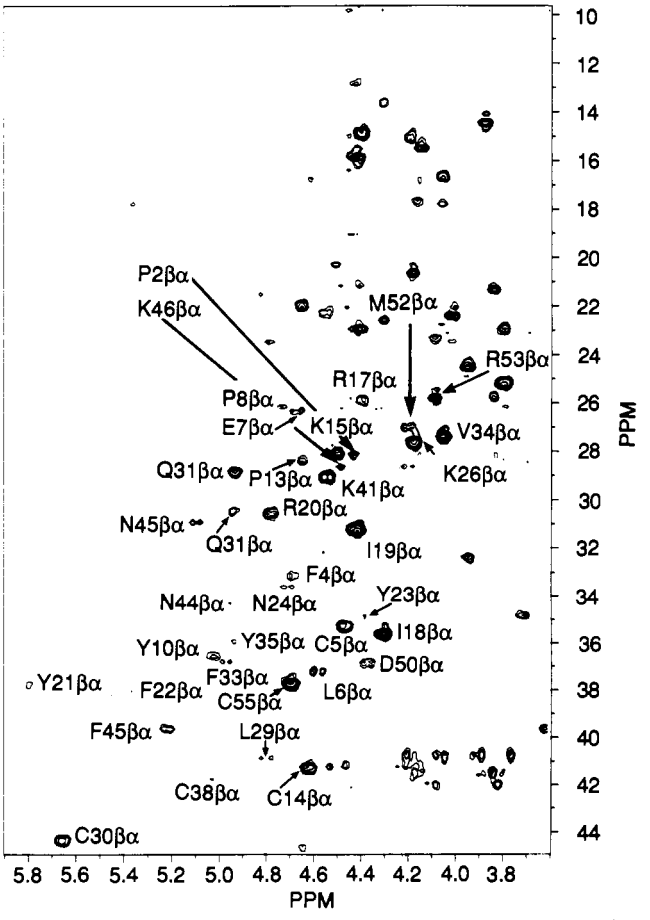

FIGURE 3: HMBC NMR natural abundance spectrum of the Hα,Cx region.

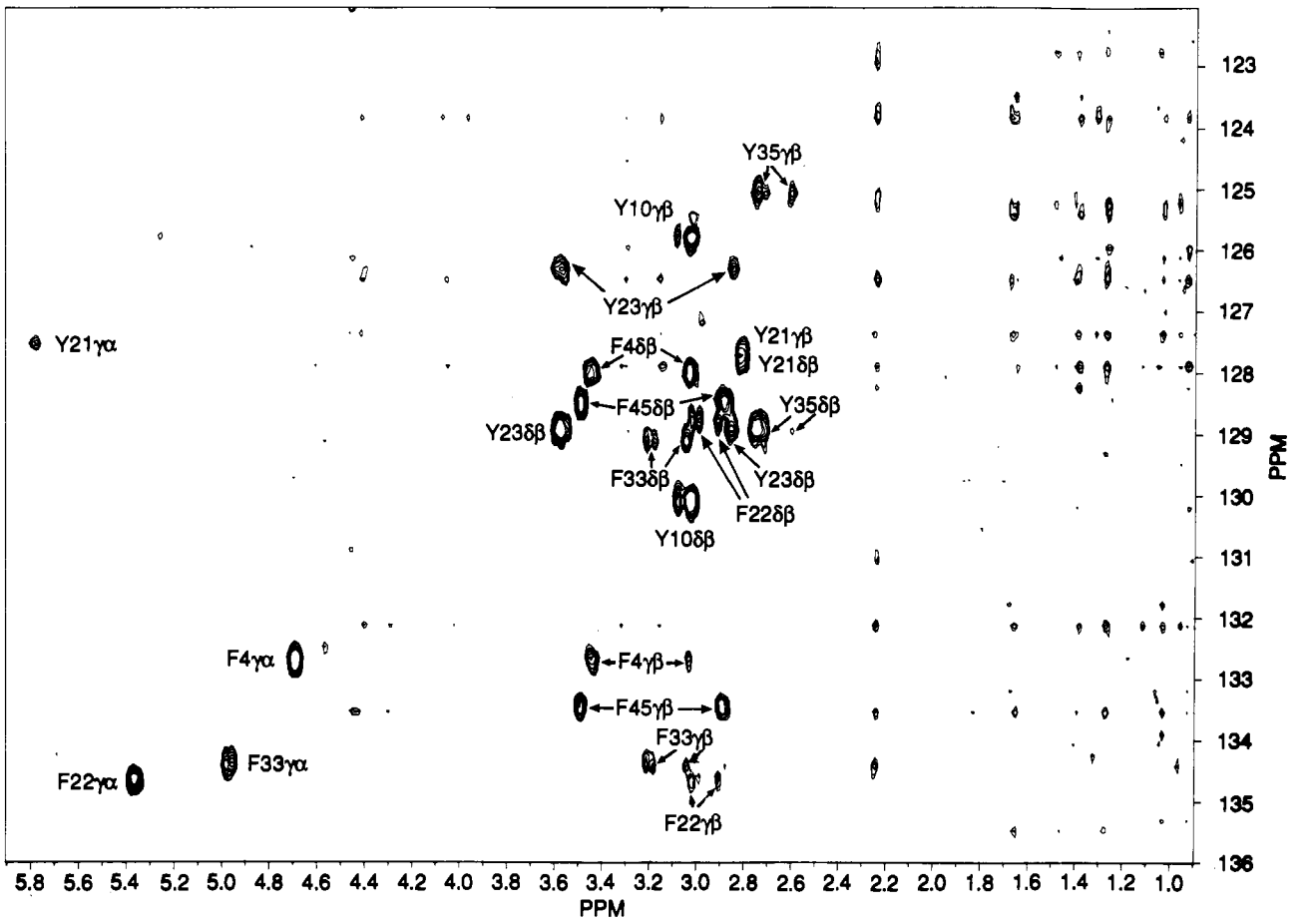

FIGURE 4: HMBC NMR natural abundance spectrum of BPTI. The Cγ and Cδ carbon resonances of the aromatic part of the spectrum. R(C-arom,Hα) and R(C-arom,Hβ) are shown.

assignments are made on the basis of both one-bond and long-range J connectivity, and the results are also summarized in Table S2.

As demonstrated recently by Davis (1989), long-range carbon–hydrogen couplings provide an extremely simple and effective handle for assignment of the aromatic carbons, especially the quaternary ones. For rapidly flipping tyrosine and phenylalanine rings, with equivalent Cδ (and Cε) resonances, a triplet-like pattern is observed for the Cδ and Cε carbons (Figure S1, Supplementary Material). The center of the triplet originates from $^3J(C\delta,H\delta')$ or $^3J(C\epsilon,H\epsilon')$ couplings, which are invariably quite large (6–8 Hz) (Ernst et al., 1977). The outer lines are due to one-bond J correlation. Note that the $^1J(C,H)$ correlations in the aromatic region of the spectrum are significantly stronger for a multiple-quantum excitation delay of 35 ms (maximum excitation for J = 157 Hz, zero excitation for J = 143 Hz or J = 171 Hz) compared to the spectrum recorded with a 38-ms delay.

$^2J(C,H)$ tends to be small in aromatic compounds (<3 Hz) with the exception of $^2J(C\zeta,H\epsilon)$ in tyrosines. Correlations originating from other two-bond J couplings are very weak or absent. The $^2J(C\zeta,H\epsilon)$ couplings in tyrosines are anomalously large because the OH substiuent makes the coupling more negative and hence increases its absolute value. Combining the spectrum, Δ_2 = 35 ms (Figure S1, Supplementary Material), with the spectrum recorded with a 38-ms excitation delay and using R(C-arom,Hα,β) (Figure 4) a nearly complete set of assignments for the aromatic carbons is obtained (Table S2).

^1H Chemical Shifts. Nearly complete ^1H chemical shift assignments have previously been reported by Wagner and Wüthrich (1982) and Wagner et al. (1987). The HMBC technique provides extensive double checks for these proton assignments and allowed additional assignments to be made for residues Lys-15, Lys-26, and Arg-39. The position of Lys-15 Hδ is ensured through the observation of R(Cε,Hδ), R(Cγ,Hδ), and of R(Cβ,Hδ). For the Hε resonance R(Cε,Hε), R(Cδ,Hε) and R(Cγ,Hε) are observed. For Lys-26 Hδ, resonances similar to Lys-15 are observed. For Arg-39 Hγ, and R(Cβ,Hγ) and R(Cγ,Hγ) resonances are observed. The ^1H chemical shifts for Lys-46 Hδ is in our study observed at 1.85 ppm on the basis of the observation of R(Cγ,Hδ) and R-(Cβ,Hδ).

Discussion

The Karplus relationship is well known for three-bond hydrogen–hydrogen couplings (Karplus, 1959). It has also been applied to carbon–hydrogen and carbon–carbon coupling constants, and inherent problems especially for very small dihedral angles have been pointed out (Barfield, 1980; Hansen, 1981). However, this case is not likely to occur in proteins, and three-bond couplings can therefore be used to obtain structural information. Expected values for the $^3J(C',H\beta)$ trans and gauche geometries in various types of amino acids are available (Hansen et al., 1975; Espersen & Martin, 1976).

The fact that intensities rather than actual magnitudes are measured in the present study combined with the possibility that a low intensity (zero intensity) may be caused by relaxation, makes it necessary to base conclusions primarily on observed resonances rather than on missing or very weak resonances. However, a missing resonance, R(Cx,Hy) can be used positively, if the effects of relaxation and passive couplings

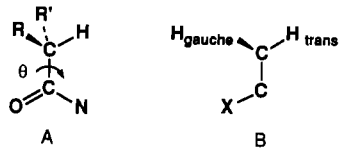

FIGURE 5: (A) $\theta = 180°$. (B) One hydrogen is gauche and the other is trans to the substituent.

can be assessed through the observation of another suitable resonance involving H*y*.

The number of observable three-bond correlations may be too small to describe the rotamers around χ_n. In order to improve this situation, two-bond carbon–hydrogen coupling constants can be used. These have been studied in, e.g., carbohydrates (Schwarcz, 1975). Additional information is obtained from studies of carbon–carbon coupling constants (Hansen et al., 1977) as the trends found for carbon–carbon couplings may be transferred to carbon–hydrogen couplings (Hansen & Berg, 1983). Two different situations, one relating to the C′ carbons (Figure 5A) and the other to Cα and other side-chain carbons (Figure 5B), are shown. An electronegative substituent gives a positive contribution to the coupling if the hydrogen and the electronegative substituent are in a trans position and a negative contribution if they are cis or gauche. As ^2J(C,H) usually is negative, a substituent gauche or cis to X will therefore lead to numerically larger coupling constants and thus make resonances detected via two-bond couplings more easily observable.

Thus, ^nJ(C,H), n = 2 or 3, can be of great use in categorizing the types of side-chain conformations through comparisons of intensity patterns. For this purpose, the side chains can be divided into classes according to their number of aliphatic carbons in the chain. The χ_1, χ_2, etc. angles can in principle be determined in the same way. However, in some cases the analysis may be hampered due to passive couplings to protons on the next carbon along the chain.

$^3J(C',H\beta)$. This type of coupling is observed for 21 carbonyl carbons (Figure 1). For most residues only a single resonance corresponding to coupling to one of the two β-hydrogens is observed, confirming that the gauche coupling is small. Consequently, rotamer type 3 (Figure 6A) does not give rise to any observable resonances. Furthermore, R(C′,Hβ) intensities for type 1 and type 2 residues of AMX type may be compared as the passive coupling pattern (see Figure 6) is the same for these two types of rotamers. If rotamer averaging takes place both ^3J(C′,Hβ) couplings may in principle become sufficiently large enough to yield correlations to both Hβ resonances. The only case where two resonances are observed is Gln-49. However, as discussed below a skew rotamer is also compatible with the observation of two R(C′,Hβ) resonances. For residues with protons at the γ-carbon, only a few R(C′,Hβ) correlations are observed. Those are Lys-26 and Arg-17, both having identical β chemical shifts, and therefore more easily observed as discussed previously. Resonances of residues with nonequivalent β-protons, Gln-31 and Gln-49, are also observed. Only few such R(C′,Hβ) correlations are observed for residues with long side chains because of attenuation caused by passive couplings to γ-protons. Arg-39, which is assigned a type 2 residue (Wagner et al., 1987), is not observed.

$^2J(C\alpha,H\beta)$. This two-bond coupling depends on the dihedral angle between the NH group and the β-hydrogens as described in general previously. It will only give rise to strong resonances when the NH group is gauche or cis to a β-hydrogen. We can therefore expect that Hβ_3 will give rise to one resonance in type 1 and Hβ_2 to one resonance in type 3, whereas both hydrogens will show resonances in type 2 as both hydrogens are gauche to the NH group in this rotamer (see Figure 6). All Ala's show strong resonances. Most residues show a single R(Cα,Hβ) resonance. Residues showing two R(Cα,Hβ) resonances are Tyr-23, Cys-30, Tyr-35, and Gln-49. This is consistent with the previous classification of these residues as type 2 (Wagner et al., 1987). However, the two resonances generally differ in intensity. This difference in intensity can result from two separate effects. First, the passive ^3J(Hα,Hβ) couplings are different and therefore influence the intensities differently according to eq 1. In the latter case, Hβ_3 is expected to be weaker than the Hβ_2 resonance. Secondly, the rotamer may be slightly skew as depicted in 2a or 2c in Figure 6B,C, leading to one coupling constant, ^2J(Cα,Hβ) being larger than the other and hence one intensity being larger than the other. In that case it can be determined which hydrogen the NH group is closest to, as the couplings grows larger the closer a cis situation is approached. For 2c the resonance, R(Cα,Hβ_3), is the most intense, and, for 2a, R(Cα,Hβ_2) is the most intense (vide infra). The important point is that the observation of two resonances is a strong indicator of a type 2 rotamer.

Cys-51 is characterized as type 2 by Wagner et al. (1987), but Cys-51 shows only one resonance. Arg-39 has identical Hβ chemical shifts and shows therefore only one resonance. Of the rotamers previously characterized as type 1 or type 3, Phe-4, Phe-22, Gln-31(weak), Phe-33, Arg-42(weak), Asn-43, Phe-45, and Cys-55 are observed. Thr-11 and Thr-54 are very weak and Cys-38 is absent. In addition we observe clear correlations for the nonclassified residues Cys-5, Tyr-10, Arg-17, Lys-26, Asn-44, Ser-47, and Asp-50. In general, the types of residues most easily observed are Phe, Tyr, Asp, Asn, Cys, and Ser because of the absence of γ-hydrogens, whereas Thr, Ile, and Val show very weak resonances due to the large number of γ-hydrogens. Similarly, it can be expected that residues like Glu, Gln, Lys, Pro, Met, and Arg will show weaker intensities for R(Cα,Hβ) resonances. The resonances of Lys-26 and Arg-39 are present, but these have identical β-hydrogen chemical shifts with no passive ^3J(Hα,Hβ) couplings and therefore increased intensity.

$^2J(C\beta,H\alpha)$. This type of two-bond coupling is normally small due to the nitrogen substituent at the α-carbon (Karabatsos, 1965). An electronegative substituent at the β-carbon may, however, counteract this effect in analogy with ^2J(Cα,Hβ). The use of ^2J(Cβ,Hα) couplings for conformational studies can be nicely demonstrated for cysteines. The cysteines show a substantial spread in intensities from the very weak (Cys-38) to the very strong (Cys-55) (Figure 3). A very strong resonance (large ^2J) is only expected in the optimal case in which the sulfur is gauche to the the α-proton (type 2 and 3, R = S). Observation of no resonance at all could point toward a type 1 as in case of Cys-38. Observation of a resonance does not distinguish between types 2 and 3, and other couplings are needed in this case. Other residues in which ^2J(Cβ,Hα) can be large are Thr and Ser, whereas cases with nonelectronegative substituents at the β-carbon usually have too small couplings to be observable. This is also the case for Phe and Tyr residues.

$^3J(C\gamma,H\alpha)$. Residues with γ-carbons are numerous, so this type of coupling can in fact occur in most residues. Large ^3J(Cγ,Hα) couplings are expected for type 1. Examples are seen for Phe-4, Phe-22, and Phe-33 (Figure 4). Observation of this type of resonance is a strong indicator of a type 1 rotamer.

Side-Chain Conformations. Combining the coupling constant information ^3J(C′,Hβ), ^2J(Cα,Hβ), ^2J(Cβ,Hα), and

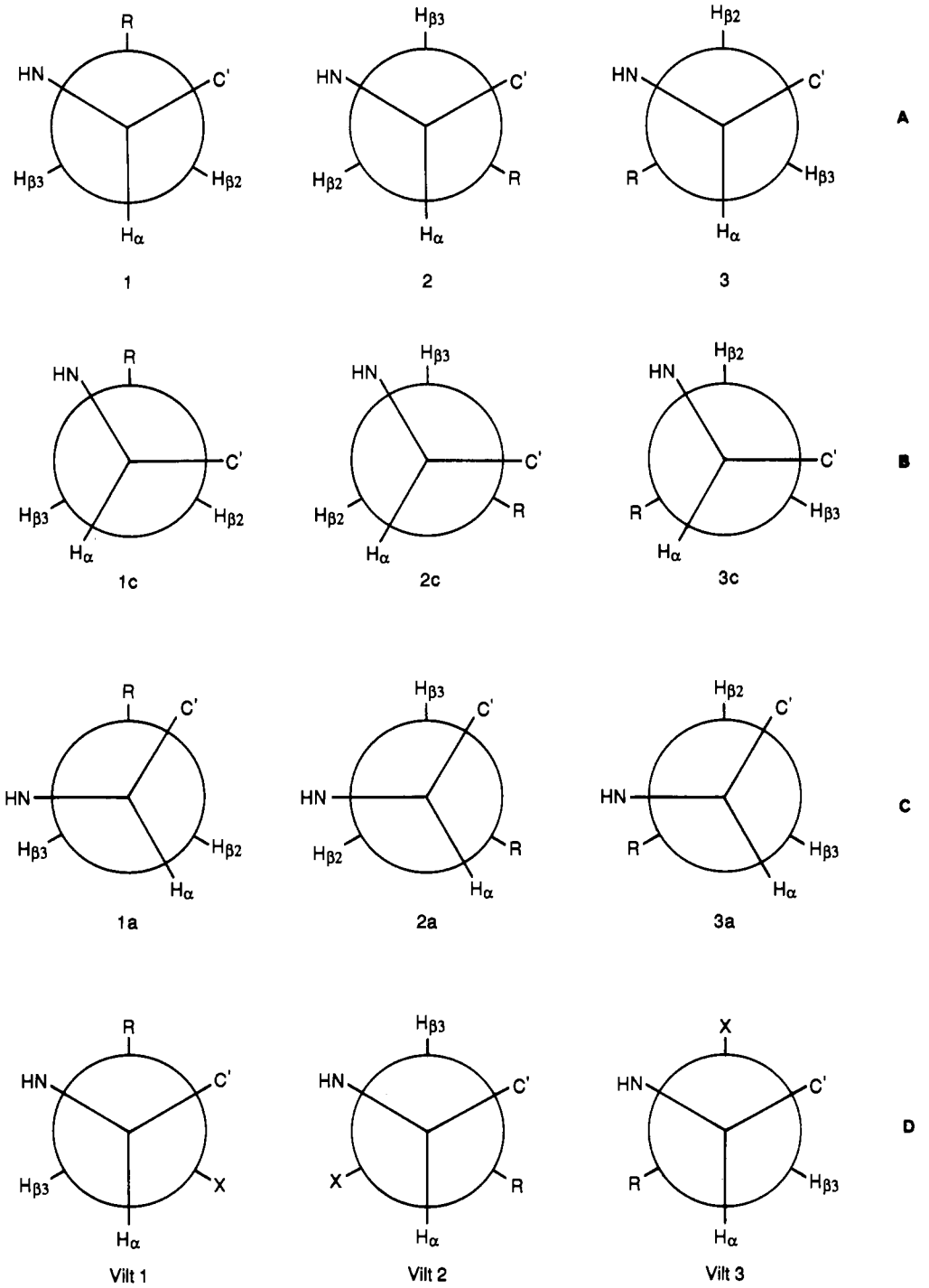

FIGURE 6: Rotamers around the Cα–Cβ bond (χ_1 angle). (A) The standard rotamers are referred to as types 1, 2, and 3. (B) and (C) Skew rotamers are 1c, 2c, and 3c (clockwise) and 1a, 2a, and 3a (anticlockwise). (D) Val, R = X = CH_3; Ile, R = CH_3, X = CH_2CH_2; Thr, R = CH_3, X = OH. The Vilt structures exist as skew structures Vilt 1c, Vilt 1a, etc., in a manner analogous to rotamers 1, 2, and 3.

^3J(Cγ,Hα) gathered from intensities, the side-chain conformations can be classified according to types 1–3 (Figure 6). The possibility that free rotation can occur around the Cα–Cβ bond should always be considered a possibility. For a number of residues such a classification previously was made on the basis of ^3J(Hα,Hβ) coupling constants and NOE effects (Wagner et al., 1987). The rotamers are depicted in Figure 6, and the expected resonance patterns are given in Chart I, including resonances based on ^3J(Hα,Hβ) coupling constants. The patterns are seen to be unique for each type of rotamer.

For example, typical rotamer 1 type patterns are observed for Phe-4, Phe-22, and Phe-33, which show the following intensity pattern: one R(C′,Hβ) resonance and one R(Cα,Hβ) resonance are observed at the same ^1H chemical shift. Furthermore, one resonance R(Cγ,Hα) is strong and R(Cβ,Hα) is weak [for a number of residues this intensity leads to no coupling constant information (see above)].

A typical type 2 pattern (Chart I) is observed for Tyr-23, which shows one R(C′,Hβ) resonance, two R(Cα,Hβ) resonances (for a discussion of intensities see above), one R(Cβ,Hα) resonance, and no R(Cγ,Hα) resonance. A R(Cβ,Hα) resonance may also be observed if the substituent at the β-carbon is electronegative.

Type 3 looks as follows. Resonances R(C′,Hβ) and R(Cγ,Hα) are not observed. One R(Cα,Hβ) resonance is expected but may be weak in residues with a γ-carbon, and one

Table I: Assignment of Rotamer Types of the Cα–Cβ Bond[a] and Stereospecific Assignments of β-Hydrogens

residue	assign.	lit assign.[b]	X-ray[c]	dihedral angles	stereospecific assign. (ppm)
Phe-4	1	1	1	51.1, 154.1	$\delta H\beta_3 = 2.99$
Cys-5	3		3	−73.8, 40.7	
Tyr-10	2 or 3		2	−67.2, −179.4	
Arg-20	3[d]		3	−66.5, 41.8	
Phe-22	1[k]	1	1	−153.5, 75.2	$\delta H\beta_3 = 2.95$
Tyr-23	2	2	2	−69.2, 174.5	$\delta H\beta_2 = 2.75$
Asn-24	2c		2	−71.3, 178.2	$\delta H\beta_2 = 2.18$
Cys-30	*e*	2	3	56.6, −65.2	
Gln-31	3[d]	3	3	−61.1, 47.4	
Phe-33	1	1	1	88.6, −156.0	$\delta H\beta_3 = 3.15$
Tyr-35	2c	2	2	−74.9, 166.5	$\delta H\beta_2 = 2.52$
Cys-38	*f*	1	1	62.2, −176.0	
Arg-39	3[g]	2	3	−70.4, 57.4	
Arg-42	*h*	3	3	29.3, −73.0	
Asn-43	2c[i]		2	−55.5, −164.6	$\delta H\beta_2 = 3.35$
Asn-44	2c[i]		2	−54.5, 175.0	
Phe-45	3	3	3	−65.1, 46.6	$\delta H\beta_2 = 2.80$
Gln-49	2a	2	3	36.5, −60.3	$\delta H\beta_2 = 2.0$
Asp-50	1a		3	−87.6, 16.5	$\delta H\beta_3 = 2.73$
Cys-51	*e*	2	2	170.8, −72.7	
Met-52	*e*	2	3	−66.3, 49.1	
Cys-55	*e*	3	3	39.1, −71.0	

[a] See Figure 6. [b] Wagner et al. (1987). [c] Taken from Wlodawer et al. (1987). Skewness is not given, as not all rotamers are ideal. See dihedral angles. [d] Difficult to support positively (see text). [e] Not assignable on the basis of present evidence. [f] Overlapping resonances make identification uncertain. [g] Identical Hβ chemical shifts. [h] See text. [i] Very skew structure. [j] Assignments based on carbon–hydrogen coupling constants. [k] Most likely a skew structure (see discussion).

Chart I: Resonance Patterns of Rotamers around the Cα–Cβ Bond

	1	2	3	1c	2c	3c	1a	2a	3a
R(C′,Hβ$_2$)		+			w	w[b]		w	w[b]
R(C′,Hβ$_3$)	+		w				w		
R(Cα,Hβ$_2$)		+[c]	+[d]			s[e]		s[e]	
R(Cα,Hβ$_3$)	+	+			s[e]		s[e]		
R(Cγ,Hα)	+			w			w		
R(Cβ,Hα)		+[a]	+[a]			s[a]		s[a]	
^3J(Hα,Hβ$_2$)	sm[f]	sm	l	sm	m	m	m	sm	m
^3J(Hα,Hβ$_3$)	sm	l	sm	m	m	m	sm	m	m

[a] Particularly strong if R is an electronegative substituent like OH, OR, or SH. [b] w means weak, possibly observed if the skewness is strong. [c] Stronger than R(Cα,Hβ$_3$), because of large passive Hα,Hβ coupling. [d] Could be weakened by large passive Hα,Hβ$_2$ coupling. [e] s means strong. The resonance is stronger because of the nearly cis arrangement of NH and Hβ. Furthermore, the passive Hα,Hβ coupling is diminished compared to the classic structures. [f] sm means small, m means medium, and l means large. [g] Not observed for Thr.

R(Cβ,Hα) resonance is likewise expected, providing the γ-substituent is electronegative. The positive evidence to pick a type 3 rotamer on grounds of carbon–hydrogen couplings alone is therefore limited.

The rotamer assignments are given in Table I and are compared with those based on ^1H data. The agreement is generally very good.

Finally, the case of skewed rotamers must also be considered. Asn-43 and Asn-44 represent type 2 cases that are both very skew (2c in Figure 6B). The great skewness results in the fact that only one R(Cα,Hβ) resonance is observed. However, the Hβ involved is not the same as that of R(C′,Hβ). This pattern is unique. Gln-49 refers to a different skew type called 2a. The fact that the CO group is relatively close to Hβ$_3$ means that both R(C′,Hβ$_2$) and R(C′,Hβ$_3$) can be observed together with one R(Cα,Hβ). The other R(Cα,Hβ) resonance is very weak. The description given for Gln-49 comes very close to that expected for a side chain with free rotation, but the possibility that the data could also fit a mixture of rotamers cannot be excluded. Skewed type 1 rotamers are not easily identified. However, Asp-50 represents such a case. The fact that R(C′,Hβ) and R(Cα,Hβ) are observed for the same Hβ resonance suggests a skewed structure of type 3c (Figure 6B). For some cases the additional information from ^3J(Hα,Hβ) would be helpful. An example is Phe-22 (Figure 2 and Table I). This is assigned a type 1 by Wagner et al. (1987). The resonances due to carbon–hydrogen couplings are the following, one R(Cα,Hβ$_3$), one R(C′,Hβ$_3$), and one R(Cγ,Hα) (Figure 4), clearly pointing toward a type 1 rotamer. The fact that ^3J(Hα,Hβ$_3$) is significantly smaller than ^3J(Hα,Hβ$_2$) indicates that Phe-22 is a skewed rotamer of type 1a.

Chart II: Resonances of Rotamers of Valine and Isoleucine around the Cα–Cβ Bond

	Vilt 1	Vilt 2	Vilt3
R(C′,Hβ$_3$)	+		
R(Cγ[a],Hα)	+		
R(Cγ′,[b]Hα)			+
R(Hα,Hβ$_3$)		l	

[a] For Val and Ile, R = CH_3. [b] For Val, X = CH_3; for Ile, X = CH_2CH_3.

Val, Ile, and Thr have only one β-hydrogen, and carbon–hydrogen couplings are invaluable in the determination of the rotamer distribution (Hansen et al., 1975). Both Val and Ile have two Cγ carbons. When the information from ^3J(C′,Hβ), ^3J(Cγ,Hα), ^3J(Cγ′,Hα), and ^3J(Hα,Hβ) is combined, the rotamers can be classified as demonstrated in Chart II and Figure 6D. Vilt1 is most easily identified on the basis of ^3J(Hα,Hβ), whereas Vilt2 and Vilt3 can be identified by ^{3}R-(C′,Hα) and ^{3}R(Cγ′,Hα) connectivities.

The above-mentioned rules are illustrated for Val-34. Val-34 has two γ-carbons, and both show weak R(Cγ,Hα) resonances. One is stronger than the other. R(C′,Hβ) and R(Cα,Hβ) are not observed, possibly because of the presence of six identical γ-protons. These findings can best be explained by a structure like Vilt 1a (Figure 6D), but free rotation cannot be excluded. Ile-18 and Ile-19 show no ^3J(C′,Hβ) couplings but weak ^3J(Cγ′,Hα), pointing toward a structure like Vilt 2 (Figure 6D). In this structure Hα and Hβ are antiperiplanar.

The two threonines, Thr-11 and Thr-54, show a strong R(Cβ,Hα) that together with a weak or not observed R-(C′,Hβ) and R(Cγ,Hα) resonances point very strongly toward a Vilt1 structure (Figure 6D). This is also supported by the finding of a large ^3J(Hα,Hβ) (Wagner et al., 1987). For

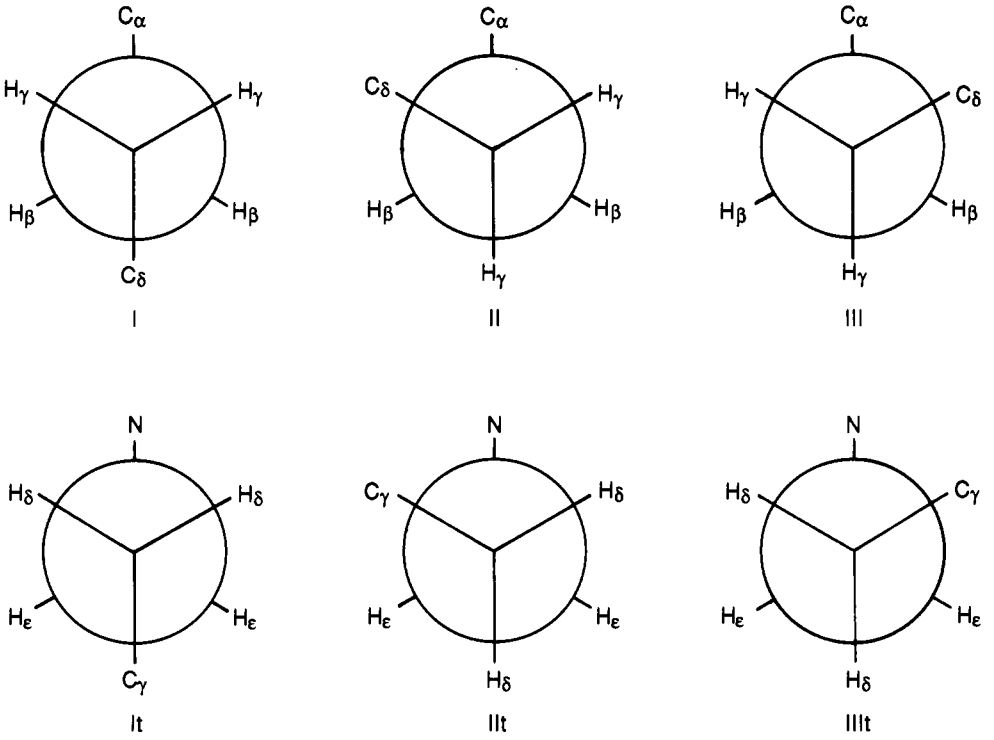

FIGURE 7: Rotamers around the Cβ–Cγ bond (χ_2 angle) and around the Cδ–Cε bond (χ_4 angle) for Lys. Skew rotamers of types a and c can be constructed as in Figure 6.

Thr-32 no strong resonances are observed at all, a result that may indicate free rotation of this side chain.

The analysis of the χ_1 angle demonstrates that ^2J(C,H) and ^3J(C,H) are very useful. Several factors should be kept in mind. Passive $^3J(H\alpha,H\beta)$, $^2J(H\beta,H\beta')$, and $^3J(H\beta,H\gamma)$ couplings influence the intensities, T_2 relaxation may be important, and the possibility of rapidly averaging multiple conformers should always be considered. The same principles can now be used to analyze the χ_2 angle. The most important difference is the larger number of hydrogens usually found at the β- and γ-carbons as well as at the adjacent carbons.

In principle, four types of coupling constants can be used, $^3J(C\alpha,H\gamma)$ and $^3J(C\delta,H\beta)$ as well as $^2J(C\beta,H\gamma)$ and $^2J(C\gamma,H\beta)$. The latter two are less useful unless an electronegative substituent is present like at the Cγ carbon of Met. Determination of χ_2 can be illustrated in the Glu and Gln residues. We are now dealing with a CH_2–CH_2 system. The rotamers are shown in Figure 7, and neither Cβ nor Cγ have electronegative substituents. The analysis presented below hinges on the two three-bond couplings $^3J(C\alpha,H\gamma)$ and $^3J(C\delta,H\beta)$. $^3J(C\alpha,H\gamma)$ follows a regular Karplus relationship (De Marco & Llinas, 1979). $^3J_{tr}$ and $^3J_{cis}$ are of the same magnitude as found for $^3J(C',H\text{-}\beta)$ and can therefore lead to observable resonances.

Glu-31 shows very small intensities for both $^3R(C\delta,H\beta_2)$ and $^3R(C\delta,H\beta_3)$ as well as for $R(C\alpha,H\gamma_1)$ and $R(C\alpha,H\gamma_2)$ pointing strongly toward structure I (Figure 7). The findings for Gln-49 are somewhat different. $^3R(C\delta,H\beta)$ shows two resonances of unequal intensity (Figure 1), whereas $^3J(C\alpha,H\gamma)$ gives rise to resonances of almost equal intensities. A $^3J(C,H)_{gauche}$ is not expected to give rise to a resonance, as discussed previously. One way to explain the observation of two sets of two resonances due to three-bond carbon–hydrogen couplings is by assuming a skewed rotamer of type IIIc (Figure 7A). Free rotation is another possibility, which is discussed later. The Glu and Gln residues constitute favorable cases as the Hβ hydrogens have different chemical shifts and so do the Hγ hydrogens.

Instead of discussing each χ angle, a more general approach can be taken comparing the intensity patterns for the entire side chain using the intensities as a fingerprint. Such a search is useful for the fully extended chain except that this mainly will show weak or absent resonances. A consistent picture of weak resonances throughout the chain could help to confirm the fully extended form. Another standard geometry to be found is that of a Glu forming a hydrogen bond between the δ-carboxyl group and its own backbone NH group. Such an arrangement has been suggested for Gln-49 in solution on the basis of titration studies (Wagner et al., 1987). It is apparent from the previous discussion that the pattern observed for Gln-49 is different from those of the other Glu and Gln residues. Wagner et al. (1987) suggested a type 2 rotamer. The present data favor a type 2a rotamer (Figure 6). Model studies, on the other hand, suggest that this kind of hydrogen bond can only be achieved by a combination of type 1a + a type IIIc or by a type 3c + a type IIa rotamers around the Cα–Cβ and Cβ–Cγ bonds, respectively. A type 2a geometry is a possibility if the γ-COOH group forms a hydrogen bond to the previous CO backbone carbonyl group. A flexing of the eight-membered ring formed by hydrogen bonding could lead to an averaging of type II and type III rotamers around the Cβ–Cγ bond, in good agreement with observed resonances.

Stereospecific Assignments. Knowing the three-bond $^3J(H\alpha,H\beta)$ coupling constants, the stereospecific assignments can be made using $^3J(C',H\beta)$ couplings (Hansen et al., 1975). For residues of type 3 no three-bond carbon–hydrogen couplings are observed. The stereospecific assignment must therefore be based on resonances due to two-bond carbon–hydrogen coupling constants, $^2J(C\alpha,H\beta)$. For those residues not characterized by hydrogen–hydrogen couplings, stereospecific assignments can be done solely on the basis of carbon–hydrogen coupling constants in the following cases. Type 1 can be assigned by means of $^3J(C\gamma,H\alpha)$ (see Chart I), and $^3J(C',H\beta)$ can be used for stereospecific assignment. If two $R(C\alpha,H\beta)$ resonances are observed, a type 2 is assigned and $R(C',H\beta)$ can be used for stereospecific assignment. However,

in most cases a combination of H,H and C,H couplings is the best way of making stereospecific assignments. Stereospecific assignments are illustrated for Hβ protons but are not restricted to those.

Conclusions

The use of long-range carbon–hydrogen coupling constant information as estimated from HMBC resonance intensities can lead to a complete assignment of the natural abundance ^{13}C spectrum of a protein (BPTI). The multitude of couplings to one carbon ensures a consistent set of assignments. The combined use of both ^1J(C,H) and ^nJ(C,H) turns out to be very useful. In case of overcrowding of the spectrum resonances due to ^1J(C,H) can easily be faded out by adjustment of Δ_2. The assignment of the ^{13}C spectrum does also lead to the assignment of the ^1H spectrum, and especially the tightly coupled parts of the ^1H spectrum are often more easily approached this way. The intensities in the spectrum depends on ^nJ(C,H), ^nJ(H,H), and T_2 relaxation. The influence of the latter may be judged from intensity comparisons of the various carbons detected via the hydrogen in question. The effects of passive homocouplings are constants for a constant geometry and can therefore be estimated and as long as comparisons are made within one group of residues with similar geometry this is relatively straightforward. Taking these precautions ^nJ(C,H) can yield stereospecific assignments as well as conformational information both about χ, ϕ, and ψ angles. However, the ideal approach combines analysis of hydrogen–hydrogen and carbon–hydrogen coupling constants. This is particularly true for χ_2 and χ_3 angles.

Acknowledgments

I thank Dr. Ad Bax, NIH, warmly for recording the spectra and for his great help and solid advice during the preparation of the manuscript.

Supplementary Material Available

One figure showing a spectrum of the R(C-arom,H-arom) region and two tables giving ^{13}C NMR chemical shifts (6 pages). Ordering information is given on any current masthead page.

References

Barfield, M. (1980) *J. Am. Chem. Soc. 102*, 1–10.
Bax, A. (1989) *Annu. Rev. Biochem. 58*, 223–256.
Bax, A., & Summers, M. F. (1986) *J. Am. Chem. Soc. 107*, 2821–2822.
Bax, A., & Marion, D. (1988) *J. Magn. Reson. 78*, 186–191.
Bax, A., Sparks, S. W., & Torchia, D. A. (1988) *J. Am. Chem. Soc. 110*, 7926–7927.
Bermel, W., Wagner, K., & Griesinger, C. (1989) *J. Magn. Reson. 83*, 223–232.
Braunschweiler, L., & Ernst, R. R. (1983) *J. Magn. Reson. 53*, 521–528.
Bystrov, V. F. (1976) *Prog. Nucl. Magn. Reson. Spectrosc. 10*, 41–81.
Bystrov, V. F., Gavrilov, Y. D., & Solkan, V. N. (1975) *J. Magn. Reson. 19*, 123–129.
Clore, G. M., & Gronenborn, A. M. (1987) *Protein Eng. 1*, 275–288.
Clore, G. M., & Gronenborn, A. M. (1989) *CFC Crit. Rev. Biochem. Mol. Biol. 24*, 479–564.
Clore, G. M., Bax, A., Wingfield, P., & Gronenborn, A. M. (1988) *FEBS Lett. 238*, 17–21.
Davis, D. G. (1989) *J. Am. Chem. Soc. 111*, 5466–5468.
Davis, D. G., & Bax, A. (1985) *J. Am. Chem. Soc. 107*, 2820–2828.
De Marco, A., & Llinas, M. (1979) *Biochemistry 18*, 3846–3854.
Deisenhofer, J., & Steigeman, W. (1975) *Acta Crystallogr. B31*, 238–250.
Driscoll, P. C., Gronenborn, A. M., & Clore, G. M. (1989) *FEBS Lett. 243*, 223–233.
Egli, H., & von Philipsborn, W. (1981) *Helv. Chim. Acta 64*, 976–988.
Ernst, L., Wray, V., Chertkov, V. A., & Sergeev, N. M. (1977) *J. Magn. Reson. 25*, 123–139.
Espersen, W. G., & Martin, R. B. (1976) *J. Phys. Chem. 80*, 741–745.
Guntert, P., Braun, W., Billeter, M., & Wüthrich, K. (1989) *J. Am. Chem. Soc. 111*, 3997–4004.
Hansen, P. E. (1981) *Prog. Nucl. Magn. Reson. Spectrosc. 14*, 175–296.
Hansen, P. E., & Berg, A. (1983) *Spectrosc. Int. J. 2*, 1–21.
Hansen, P. E., Feeney, J., & Roberts, G. C. K. (1975) *J. Magn. Reson. 17*, 249–261.
Hansen, P. E., Poulsen, O. K., & Berg, A. (1977) *Org. Magn. Reson. 11*, 649–658.
Karabatsos, G. J., & Orzech, C. E., Jr. (1965) *J. Am. Chem. Soc. 87*, 560.
Karplus, M. (1959) *J. Chem. Phys. 30*, 11–15.
Kessler, H., Griesinger, C., Lautz, J., Müller, A., van Gunsteren, W. F., & Berendsen, H. J. C. (1988a) *J. Am. Chem. Soc. 110*, 3393–3396.
Kessler, H., Anders, U., & Gemmecker, G. (1988b) *J. Magn. Reson. 78*, 382–388.
Kessler, H., Schmeider, P., & Bermel, W. (1990) *Biopolymers 30*, 465–475.
March, K. L., Maskalick, D. G., England, R. D., Friend, S. H., & Gurd, F. R. N. (1982) *Biochemistry 21*, 5241–5251.
Richarz, R., & Wüthrich, K. (1978) *Biochemistry 17*, 2262–2269.
Schwarz, J. A., Cyr, N., & Perlin, A. S. (1975) *Can. J. Chem. 53*, 1872–1875.
Stockman, B. J., Reily, M. D., Westler, W. M., Ulrich, E. L., & Markley, J. L. (1989) *Biochemistry 28*, 230–236.
Tüchsen, E., & Hansen, P. E. (1988) *Biochemistry 27*, 8568–8576.
Wagner, G., & Wüthrich, K. (1982) *J. Mol. Biol. 155*, 347–366.
Wagner, G., & Brühweiler, D. (1986) *Biochemistry 25*, 5839–5843.
Wagner, G., Braun, W., Havel, T. F., Schauman, T., Go, N., & Wüthrich, K. (1987) *J. Mol. Biol. 196*, 611–639.
Westler, W. M., Kamamoto, M., Nagao, H., Tomonaga, N., & Markley, J. L. (1988) *J. Am. Chem. Soc. 110*, 4093–4095.
Wlodawer, A., Walter, J., Huber, R., & Sjölin, L. (1984) *J. Mol. Biol. 180*, 301–329.
Wlodawer, A., Nachman, J., Gillard, G., Gallagher, W., & Woodward, C. (1987) *J. Mol. Biol. 198*, 469–480.
Wüthrich, K. (1986) *NMR of Proteins and Nuclei Acids*, Wiley, New York.
Wüthrich, K. (1989) *Acc. Chem. Res. 22*, 36–44.